CLIMA 2016 - proceedings of the 12th REHVA World Congress

volume 3

Heiselberg, Per Kvols

Publication date:
2016

Document Version
Publisher's PDF, also known as Version of record

Link to publication from Aalborg University

Citation for published version (APA):
Heiselberg, P. K. (Ed.) (2016). *CLIMA 2016 - proceedings of the 12th REHVA World Congress: volume 3*. Department of Civil Engineering, Aalborg University.

Simulation study of heat recovery from flat roof photovoltaic systems by mechanical ventilation for a wine warehouse in France

Leon Gaillard[#1], Stéphanie Giroux-Julien[#2], Kévin Taurines[*3], Christophe Ménézo[°4]

[#]*University Lyon 1, CETHIL UMR CNRS 5008*
Bât. Carnot, 9 rue de la Physique, Campus de la Doua, F-6921 Villeurbanne
[1]leon.gaillard@insa-lyon.fr
[2]stephanie.giroux@univ-lyon1.fr
[*]*INSA-Lyon, CETHIL UMR CNRS 5008*
Bât. Carnot, 9 rue de la Physique, Campus de la Doua, F-6921 Villeurbanne
[3]kevin.taurines@insa-lyon.fr
°University Savoie Mont-Blanc, LOCIE UMR CNRS 5271
Bât. Hélios, Campus Savoie Technolac, F-73376 Le Bourget-du-Lac
[4]christophe.menezo@univ-smb.fr

Abstract
We assess the potential to preheat space air and water using a prototype of photovoltaic-thermal array installed on the roof a wine warehouse in southern France. The system comprises a horizontal arrangement of conventional PV modules fitted to a novel metal structure that serves both as mechanical support and ventilation duct. The warehouse requires a steady interior air temperature of 14-18°C throughout the year. The load profile of the building is strongly affected by the mass of the vats. Simulations were performed with TRNSYS, using a combination of existing library components and a bespoke Type to model the steady state behaviour of the aspirated solar array structures. The potential for air preheating was assessed by calculating the enthalpy change due to the injection of outside air into the building. The potential for space preheating and hot water generation were found to be complementary, with hot water generation proving of interest during the portion of the year where the heating load of the building is negligible. Sensitivity of system performance to weather conditions is highlighted, and in particular the impact of wind on panel heat dissipation.

Keywords – BIPV-T; Hybrid solar collector; Large horizontal ventilated roof

1. Introduction

The integration of solar energy systems into industrial building roofs can reduce the carbon footprint of this sector through both grid feed-in and self-consumption strategies. In France in 2012, industrial and commercial zones accounted for approximately 0.7% of the total metropolitan land mass, equivalent to $3.8\text{x}10^3$ km² [1]. Horizontal rooftops included within this figure could represent a significant fraction of the current total photovoltaic (PV) capacity of the country, whilst offering the advantages of typically large individual rooftop areas and a daytime load profile of some industrial buildings which may favour onsite consumption of solar energy. From the technological perspective, further work is needed to optimize the integration of solar energy technology into buildings so that they more effectively contribute to building performance. Heat dissipation is a well known issue but it can be exploited to improve the thermal performance of the building [2]. Heat recovery from PV systems has been investigated for a large range of configurations, typically using water or air as the heat carrier fluid [3]. However, to date few examples of large-scale PVT for commercial and industrial buildings can be found in the literature [4].

Fig. 1. iNovaPVT technology demonstration supported through the project Horizon PV.

The Horizon PV project addresses the development of a rooftop RE systems involving (near-) horizontal PV arrays, which may be adapted to the energy needs of the host building through a variety of hybrid photovoltaic-thermal (PVT) configurations. The project focuses upon one technology, $\text{iNova}^{\text{PVT}}$, which has been developed specifically for large tertiary buildings (up to 10^5 m², or 10 MW_c). The main drivers behind this technology are an aim to optimise the utilisation of roof space for the integration of solar components; the development of PV technologies that offer improvements to both the electrical and thermal performance of buildings; an adaptation of solar energy technology to the specific needs of particular types of industrial buildings; and to provide solutions that are competitive with conventional energy supplies and building materials. In this paper we present a preliminary numerical analysis of a test site selected for a demonstration installation of $\text{iNova}^{\text{PVT}}$ technology, which includes space heating via direct injection of hot air water preheating during summer.

2. Description of PVT system and building characteristics

The $iNova^{PVT}$ concept was developed by EPC Solaire with the intention of retaining the advantages of their existing $iNova^{PV}$ solution for horizontal flat roof installations, using framed or unframed modules. Both products comprise a prefabricated modular support structure of parallel metal rails that are thermosoldered to avoid perforating the waterproof membrane, and onto which PV modules are attached mechanically. In the case of the PVT variant, the metal frame is modified to accommodate a rectangular air duct formed by the backsheet of the PV modules, the support rails, and a thin plate suspended between the rails a few centimetres above the roof lining. The dimensions of the ventilated duct are thus set by the separation of the rails, limited by the permissible mechanical load of the PV modules, and the position of the plate, which can be chosen to optimize heat recovery. In the case of framed modules, the plate distorted to ensure a constant duct thickness. Module frames vary between 33 and 50 mm, which allows for air gaps of thickness 28 to 45 mm.

The site chosen for the present study is a wine warehouse located in Sorgues, southern France. The demonstrator installation is shown in Fig. 1. The building comprises one main hangar 55.3 m long and 26 m wide, with a shallow roof varying from 10 to 11 m in height, plus single story offices and a small laboratory. The hangar houses several rows of 100 hl vats, containing new wine (post-vinification), which requires a year-round thermostat of 14-18°C. The site is primarily a storage facility, but has an additional low demand for hot water to clean the vats. The thermal performance of the building is somewhat aided by the substantial mass of the vats, but otherwise suffers from poor insulation, water tightness and air permeability. A project to refurbish the building was initiated in 2015 with a first phase of works to add class C insulation and a PVC air and water proof membrane to the existing roof structure. The building owners also opted to install a 140 kW_c plant. The facility was divided into two equal sized PV and PVT arrays, with the PVT system arranged into parallel branches connected to ventilation ducts and fans positioned along the spine of the roof. The system is set up to inject the air directly into building below, or to pass through an air-water heat exchanger installed on the roof, to provide space heating or water preheating depending on the needs of the building over the course of a year.

To illustrate the specific features of the wine warehouse, a simplified simulation was performed using TRNSYS. The building geometry was simplified to a single space with a shallow tilted metal roof, with solid 20 cm thick concrete walls without windows, a metal roof including 15 cm of insulation, and a standard composite floor of insulated concrete. Rather than modelling air infiltration, mechanical ventilation was included to replace 5000 m^3/h of air. The simulation was performed taking into account the thermal mass of 40 wine vats. Without the additional mass, the combined annual heating and cooling load is 180 kWh/m^2, comparable but slightly high for similar buildings in the US [5] and general figures for non-residential buildings in France [6]. This figure decreases slightly to 167 kWh/m² with the addition of the vats. The main impact of the high thermal mass is to smoothen out the daily variation in interior air temperature. As a result, the building air temperature is observed to float within the set point temperature range for many days with neither heating nor cooling. The effect is most apparent during spring and autumn seasons.

The addition of a PVT array on the roof has two main impacts: heat transfer through the roof will change due to its different composition and the radiative properties of the PV modules; and the PVT outlet air can be used when appropriate. The second of these two impacts will be considered in the following sections.

3. Numerical model of BIPV-T collector

A simplified steady-state physical model was developed to estimate the potential for heat recovery using the iNova^{PVT} concept, to predict the performance of the PV and Building Integrated PVT (BIPV-T) installation of the roof of the wine warehouse, and later facilitate the analysis of monitoring data. At the component level the model is similar to those developed by [7-9]. To simulate the variations in air and surface temperatures along a branch, the structure was divided into a stack of thin slices as illustrated in Fig. 3.

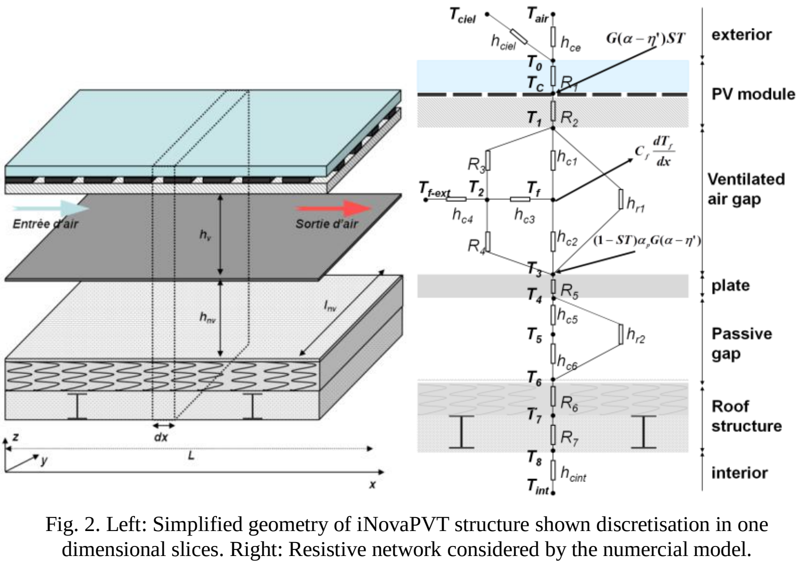

Fig. 2. Left: Simplified geometry of iNovaPVT structure shown discretisation in one dimensional slices. Right: Resistive network considered by the numercial model.

Each slice was then represented by a simple resistive network comprising 11 interconnected temperature nodes: PV modules (3 nodes for glass cover, PV cells and backsheet); ventilated air gap; suspended plate;

passive air gap; roof structure (2 layers); and the metal support rails. The model assumes that conduction in the plane of the modules is negligible and the thermal time constants of the materials are sufficiently short to ignore transient behaviour. These approximations are appropriate when considering the weak thermal coupling between adjacent modules, and when the objective is to establish the nominal performance of an array under stable operating conditions.

For each slice, an energy balance problem can be solved to obtain the local temperatures of each node by equating incident fluxes and isothermal boundary conditions (including the temperature of air in the upstream element of the ventilated duct). Adopting the symbols indicated in Fig. 2., the following set of 11 must be resolved:

$$
\begin{array}{rcl}
h_{ce}\left(T_0 - T_{air}\right) + h_{ciel}\left(T_0 - T_{ciel}\right) + \frac{1}{R_1}\left(T_0 - T_C\right) & = & 0 \\
\frac{1}{R_1}\left(T_C - T_0\right) + \frac{1}{R_2}\left(T_C - T_1\right) & = & G\left(\alpha - \eta^{'}\right) ST \\
\frac{1}{R_2}\left(T_1 - T_C\right) + \frac{1}{R_3}\left(T_1 - T_2\right) + h_{r1}\left(T_1 - T_3\right) + h_{c1}\left(T_1 - T_f\right) & = & 0 \\
\frac{1}{R_3}\left(T_2 - T_1\right) + h_{c3}\left(T_2 - T_f\right) + \frac{1}{R_4}\left(T_2 - T_3\right) + h_{c4}\left(T_2 - T_{f,ext}\right) & = & 0 \\
h_{c3}\left(T_f - T_2\right) + h_c1\left(T_f - T_1\right) + h_{c2}\left(T_f - T_3\right) & = & -C_f \frac{dT_f}{dx} \\
\frac{1}{R_4}\left(T_3 - T_2\right) + h_{r1}\left(T_3 - T_1\right) + h_{c2}\left(T_3 - T_f\right) + \frac{1}{R_5}\left(T_3 - T_4\right) & = & \left(1 - ST\right)\alpha_p G\left(\alpha - \eta^{'}\right) \\
\frac{1}{R_5}\left(T_4 - T_3\right) + h_{r2}\left(T_4 - T_6\right) + h_{c5}\left(T_4 - T_5\right) & = & 0 \\
h_{c6}\left(T_5 - T_6\right) + h_{c5}\left(T_5 - T_4\right) & = & 0 \\
h_{c6}\left(T_5 - T_6\right) + h_{r2}\left(T_6 - T_4\right) + \frac{1}{R_6}\left(T_6 - T_7\right) & = & 0 \\
\frac{1}{R_7}\left(T_7 - T_8\right) + \frac{1}{R_6}\left(T_7 - T_6\right) & = & 0 \\
\frac{1}{R_7}\left(T_8 - T_7\right) + h_{cint}\left(T_8 - T_{int}\right) & = & 0
\end{array}
, \quad (1)
$$

where the conversion efficiency of the PV cells is given by

$$\eta^{'} = \eta_{ref}\left(1 + \beta\left(T_{STC} - T_C\right) + \gamma \ln\left(\frac{G}{G_{ref}}\right)\right) = \eta^{''} - \eta_{ref}\beta T_C . \quad (2)$$

T_f represents the temperature of air in the ventilated duct, similarly T_c for PV cells, T_{air} outside air, T_{sky} the equivalent sky temperature, T_i ($0<i<8$) represent other nodes. Convective and radiative heat transfer coefficients and thermal resistances are labelled h_{ci}, h_{ri} and R_i respectively. Absorptivities of the PV cells and plate are given by α and α_p, and ST is the degree of transparency of the PV modules (unity for opaque backsheets). The system of equations can be reformulated as a conductance matrix H, and the vector of temperatures T, the product of which is equal to the vector of boundary conditions B. In this form the temperature vector can be calculated analytically by inversing the conductance matrix:

$$\mathrm{H} \cdot \mathrm{T} = \mathrm{B} \Rightarrow \mathrm{T} = \mathrm{H}^{-1} \cdot \mathrm{B} . \quad (3)$$

We thus obtain a system of equations for the vector T, including one differential equation for the variation in air temperature, which can be solved by integration to provide a relation for the air temperature as a function of position. The analytical solution is valid only for a linear system; however heat transfer coefficients depend upon node temperatures. To overcome this non-linearity, the system is resolved iteratively by successive substitution. Once the algorithm has converged for the present slice, it proceeds along the structure, adopting the output air temperature just calculated as the input boundary condition for the next element downstream. An illustration of the temperature variation in a single PVT structure is presented in Fig. 3.

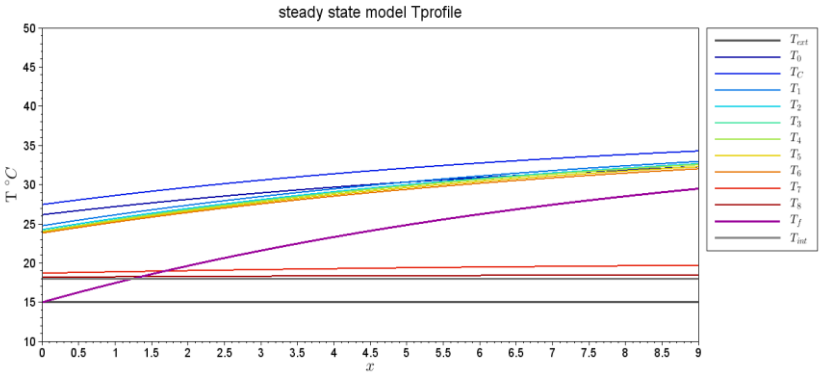

Fig. 3. Variation in steady state node temperatures along a single 9 m long ventilated branch for an incident solar radiation intensity of 500 W/m².

4. Simulation of full scale plant

The PVT collector model was incorporated into a bespoke TRNSYS Type [10] written in FORTRAN, and evoking LAPACK subroutines for matrix operations [11]. The type enabled the simulation of a single iNova^{PVT} branch as a function of imposed air flow rate and environmental conditions. For the first simulations of the full installation, the following simplifying assumptions were made: zero thermal losses in the ductwork; homogeneous environmental conditions and air flow for all branches; and the thermal interaction between the roof and PV components, was neglected.

The Meteonorm TMY dataset for the town of Orange was used in the simulation. Mechanical ventilation of the PVT array was based on the air recovery rate of the building, 5000 m^3/h, and the branches were sized for an air speed of 1m/s behind the PV modules. When considering hot water generation, the flow rate was reduced to 50%. To simulate the ordinary, unventilated iNova^{PV} arrays, the same component model was used, but assumed a constant airflow speed of 0.1m/s to account for natural stackinduced ventilation. The simulations of non-ventilated modules indicate a natural temperature difference of ~5 K between PV modules at either end of a 10 m long iNova^{PV} branch, during sunny periods with minimum wind. A first order estimation of the potential to meet the space heating need of the building was determined by considering the air replacement rate of the building and the constant thermostat schedule:

$$Q_{air} = \rho \cdot \dot{V}_{ren} \cdot C_{p,air}\left(T_{bat} - T_{ext}\right). \tag{4}$$

Where ρ is the air density (calculated using the outside air temperature), $\dot{V}_{ren}$ the air replacement rate, C_p the heat capacity of the air volume at constant pressure, T_{bat} the temperature set point (14-18°C), and T_{ext} the outside air temperature. For this estimation, the inertia arising from the building mass was neglected from the calculation. Equation (4) represents the enthalpy change that must be matched by the PVT system, which is calculated in the same manner using the outlet air temperature instead of the set point temperature.

5. Results

The performance of the system was considered for an air preheating configuration with a ventilation speed of 1m/s per branch to match the 5000m^3/h air replacement rate. The predicted variation in PV module temperatures is presented in Fig. 4. for 5th January and 2nd July. In each figure, the temperature of the first (inlet) and last (outlet) modules are shown for ventilated and unventilated branches on the east side of the roof (E1 and E10 respectively).

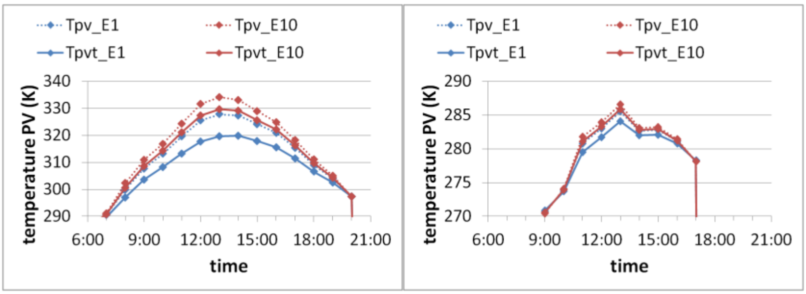

Fig. 4. Hourly temperature of ventilated (PVT) and PV branches during a summer (left) and a winter (right) day. Labels E1 and E10 represent the first and last modules of a branch.

Ventilation during the summer can cool modules at the inlet by up to 10°C, and to a lesser degree for the last modules. As a result, the PVT branches would have a slightly higher electrical performance, depending upon the interconnection architecture. The predicted cooling represents approximately 1.5 kW of heat extraction per branch. In winter the behaviour is similar by less pronounced, with 300 W of heat extraction per branch.

The potential for air heating over the course of the year is presented in Fig. 5. using the calculation introduced in section 4. The daily enthalpy change in the zone air attributed to ventilation using outside air is shown superposed with the potential gain of preheating the air using the PVT array. Enthalpy is expressed normalized by the surface area of the roof (not PVT coverage) in order to be comparable to standard measures of building energy intensity. The fractional solar coverage of the air replacement enthalpy is illustrated by a histogram in the same figure. In winter months, the potential is typically less than 20% except for sunny days with exceptionally low wind, which favours higher PV temperatures. The PVT system is rather particularly interesting during spring and autumn months, where preheating is regularly able to cover all or the majority of the air replacement heat. Note that, since the PVT system operates only during daylight hours, the instantaneous injection of heat during such days significantly exceeds the instantaneous demand. However this is acceptable given the high thermal mass of the building. For other buildings, a storage solution would need to be considered to account for the phase difference between solar production and heating load curves.

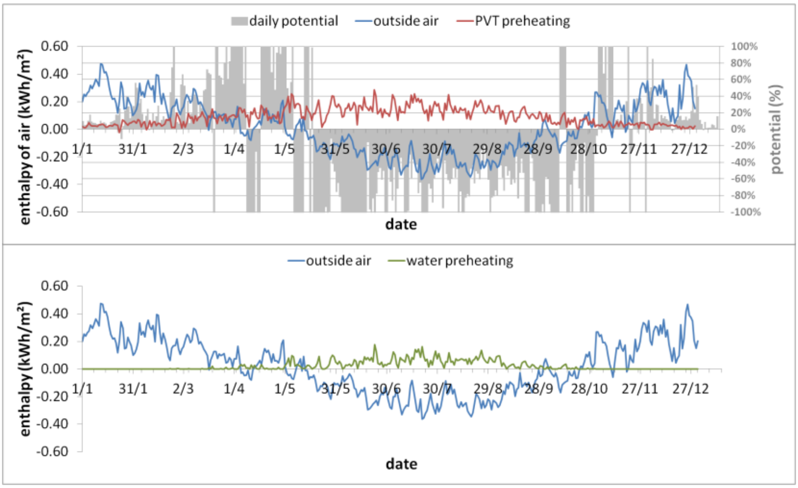

Fig. 5. Daily enthalpy change of the wine warehouse attributed to the continuous replacement of air with the exterior air. Top: potential of preheating injected air suing the PVT array. Bottom: potential of preheating water using an air-water heat exchanger mounted on the roof.

An initial estimate of water preheating potential is shown in the lower frame of Fig. 5. For this calculation, the air flow rate in the PVT array was reduced by half to 2500 m^3/h in order to increase the outlet air temperature. Preheating potential was estimated assuming the installation of a VERTIGO 2, cyclonic air-water heat exchanger operated with water from the municipal water supply at 15°C flowing at a rate of 1.3m^3/h. Under such an arrangement, a minimum air temperature of 27°C is required to transfer heat to the water circuit. The datasheet performance curve of the exchanger was used to calculate heat extraction as a function is air temperature and flow rate. At peak performance the exchanger delivers 250 kWh of water preheating capacity. The typical temperature increase of the water is 10°C.

Comparing the air and water preheating performance, it is evident that the two operational modes are complementary, with the latter being useful during the period of the year where air preheating is not required.

6. Discussion and conclusions

We have presented a preliminary simulation study of an industrial-scale PVT system comprising conventional PV modules that are mechanically ventilated on the underside by a specially modified support structure. The potential of the PVT system was considered for preheating air entering a wine warehouse to ensure a nominal air replacement rate. For the building in the study, the system was found to be particularly beneficial during spring and autumn. These gains are in addition to the primary function of electricity generation of the installation, and serve to reduce the electricity consumption due to space heating load during these periods of the year, and the production of hot water in summer. The useful extraction of heat from the PV array contributes significantly to the overall energy budget of the building and could therefore support a strategy to render the building autonomous.

Thermal performance varies considerably from one day to the next, revealing a high sensitivity to wind. A similar behaviour is observed for aspired solar walls [12]. With better insulation, the utility of the PVT preheating would presumably extend into winter months. During summer, when the building is not heated is not required, the PVT system could be connected to a hot water system through an air/water heat exchanger.

Several features have been neglected from these first simulations, and most importantly losses attributed to ductwork and thermal coupling of the PVT system to the building. These will be addressed in following work that will consider a fully integrated PVT system and building model simulation in TRNSYS. At that stage, realistic limits on HVAC capacity will also be included. The added value of the PVT system will then be evaluated in the context of other renovation measures.

Acknowledgments

The project Horizon PV was supported by the French Agency for the Environment and Energy Management (ADEME convention 1405C0042). The authors are grateful for the sustained collaboration with EPC Solaire (J.

P. Bousquet and G. Chaleyssin), manufacturer of the iNova^{PVT} system, and also the participation of the BOISSET group, owners of the wine factory site used for the prototype facility.

References

[1] Ministère de l'Ecologie, du Développement Durable et de l'Energie (MEDDE). CORINE Land Cover, level 3, large regions, http://www.statistiques.developpement-durable.gouv.fr/donnees-ligne/t/donnees.html, accessed 2015

[2] E. Skoplaki, & J.A. Palyvos. On the temperature dependence of photovoltaic module electrical performance: A review of efficiency/power correlations. Solar Energy, 83(5), 614–624.

[3] T.T. Chow. A review on photovoltaic/thermal hybrid solar technology. Applied Energy, *87*(2), 365–379. doi:10.1016/j.apenergy.2009.06.037

[4] S.A. Kalogirou, Y. Tripanagnostopoulos. Industrial application of PV/T solar energy systems, Applied Thermal Engineering. 27 (2007) 1259–1270

[5] U.S. Energy Information Administration. Commercial Buildings Sector Energy Intensities: 1992- 2003. https://www.eia.gov/emeu/efficiency/cbecstrends/cbecs_tables_list.htm, accessed 2015

[6] Agency for Environment and energy Management, (ADEME, France). Les chiffres clés du bâtiment 2013. http://www.presse.ademe.fr/2014/04/les-chiffres-cles-du-batiment-2013.html, accessed 2015

[7] A. Tiwarin & M.S. Sodha. Parametric study of various configurations of hybrid PV/thermal air collector: Experimental validation of theoretical model. Solar Energy Materials and Solar Cells. 91 (2007) 17-28.

[8] S. Bambrook. Investigation of photovoltaic/thermal air systems to creat a zero energy house in Sydney. PhD thesis (2011), University of New South Wales.

[9] K. Touafek, M. Haddadi, M. Ali. Design and modeling of a phtovoltaic thermal collector for domestic air heating and electricity prodcution. Energy and Buildings. 59 (2013) 21-28

[10] S.A. Klein et al, 2010, TRNSYS 17: A Transient System Simulation Program, Solar Energy Laboratory, University of Wisconsin, Madison, USA, http://sel.me.wisc.edu/trnsys

[11] E. Anderson, et al., LAPACK Users' Guide, Third Edition, 1999, pub. Society for Industrial and Applied Mathematics, Philadelphia, PA, ISBN 0-89871-447-8 http://www.netlib.org/lapack/lug/lapack_lug.html

[12] Sébastien Cordeau, Suzelle Barrington, Performance of unglazed solar ventilation air pre-heaters for broiler barns, Solar Energy 85 (2011) 1418-1429.